Thermal Performance and Drying Evaluation of a CFD-Optimized Biomass-Fired Fish Dryer for Various Fish Products

Monalyn L. Oloroso[1], Ginno L. Andres[2]

[1]Polytechnic University of the Philippines – Open University, Philippines, and Capiz State University, Philippines, mloloroso@capsu.edu.ph
[2]Polytechnic University of the Philippines – Open University, Philippines

Abstract
Limited studies have integrated air distribution simulation and experimental validation to improve the performance of biomass-fired fish dryers. This study aimed to optimsize and evaluate the thermal and airflow performance of a multi-layer biomass-fired fish dryer through computational fluid dynamics (CFD) analysis and experimental validation. The dryer's performance was evaluated using four fish products following the PNS/BAFS 344:2022 standards. CFD results showed that the addition of exhaust vents and four 45-degree baffles provided a more uniform airflow and temperature distribution. Experimental results indicated drying air temperatures ranging from 77.5 °C to 80.8 °C, with a mean of 78.93 °C. The highest drying rate was 18.48 kg/h for split round scad, while boneless anchovies achieved the highest heating system efficiency of 75.17%, demonstrating the dryer's potential for practical fish drying applications.

Keywords: biomass dryers; computational fluid dynamics; drying systems; fish drying; temperature uniformity

1. Introduction

Fish deteriorates within a few hours after capture; hence, the need for preservation and processing to reduce microbial decomposition and retard spoilage. Drying of fish is the most practiced processing method in the Philippines, especially for small species [1]. It was found that reducing the moisture content of fish to twenty-five percent will retard bacteria and reduce autolytic activity. The sun drying method is widely used for drying fish since it requires cheaper operating expenses. However, this method has disadvantages due to unpredictable weather conditions, resulting in uneven drying and a relatively slow drying rate, thus increasing the tendency of spoilage. Using racks for drying fish allows "well exposure of fish muscle to sunlight and moving air that makes the fish dry quickly, and the product would be clean and hygienic" [2]. Previous studies on enclosed drying systems demonstrated improved drying efficiency and product protection compared to traditional sun drying methods [3]. However, based on the study, an unsatisfactory condition was still observed in these areas that use mats and racks. Since contamination during fish processing is likely to happen, dried fish products were investigated in Bangladesh [4]. A study also revealed fungal diversity and "mycotoxin contamination among dried fish sold at the seafood market in Zhanjiang" [5].

Generally, previous studies showed that the traditional drying method of fish, which mainly uses direct sunlight as the source of heat, natural air, and racks, has many disadvantages, including low drying rates, low product quality, and health hazards. As traditional fish drying processes do not meet the food safety and health requirements following Good Manufacturing Practice (GMP), it has become necessary to design the fish drying process to produce safe and healthier food efficiently [6].Burning wood and fossil fuels as heat sources have also been practiced for fish drying in some areas. However, these processes involve high operational costs and may damage the environment and adversely impact climate [7].

Biomass can be an alternative energy to replace fossil energy [8]. In the Philippines, rice husk is one of the major biomass sources. It is a by-product of rice milling, readily available in large quantities, and easy to collect. It is a clean and environmentally friendly fuel and does not cause any pollution during combustion. It has been used successfully as a fuel in many agricultural machines – including a flatbed dryer for grains. It entails cheaper investment and operating costs. It is concluded that biomass-powered heating systems might be a good solution for fish dryer designs in terms of costs and environmental concerns. Different drying systems commonly consist of a heat source unit, an air conveying system, a drying chamber, and an air exhaust. Though the different technologies involve different designs, they encompass a common principle that hot air absorbs and conveys moisture from the product by heat and mass transfer and diffusion process, while the residual air is discharged through an exhaust unit [9].

Drying air temperature is critical in drying operations to improve efficiency and product quality. The even distribution of heat in the drying chamber is also vital in the design to minimize operations, such as turning fish trays during operation. As demonstrated in tobacco, food, and fiber dryers [10, 11, 12], non-uniform airflow results in uneven moisture removal, which degrades quality and lengthens drying time. Design modifications such as internal baffles, guide plates, swirlers, and optimized fan placements significantly improve airflow and temperature uniformity. Adding baffles in heat pump cabinet dryers improved flow uniformity by over 50% and temperature uniformity by over 85%, enhancing product quality [13, 14]. Similarly, optimizing the number and placement of air outlets and wind cones in ceramic drying rooms reduced velocity and temperature non-uniformity

coefficients by up to 23% [15]. Fan configurations with grilles or chimneys also stabilize airflow patterns and temperature fields, leading to faster drying rates and better energy efficiency [16, 17].
Computational Fluid Dynamics (CFD) based studies highlight that careful structural design and operational parameter optimization can enhance drying performance in terms of airflow and temperature distribution [11, 18, 19]. In addition, CFD has been widely used to evaluate the influence of geometric modifications, such as baffle integration, on flow transport and system performance [20].
Several studies have focused on the design and fabrication of biomass-powered multi-tray dryers for fish drying and related applications. A biomass-fueled convective dryer with stainless steel trays and indirect heat supplied by woody biomass combustion was developed, achieving thermal efficiencies of about 21–24% and demonstrating effective drying performance for products such as anchovy and shrimp [21]. In another study, a hybrid gas–biogas dryer prototype with multiple trays was designed for drying various food products, including fish, incorporating controlled airflow and temperature regulation to improve drying uniformity [22]. Additionally, a charcoal-fired cabinet-type fish dryer with a batch capacity of about 10 kg exhibited high efficiency (up to ~95% at higher fan speeds) and uniform heat distribution across trays, indicating effective multi-tray drying performance [23].

There is a need to scale up designs to industrial levels, as the majority of current prototypes concentrate on small to medium-scale capacities [21, 24]. Furthermore, current biomass-powered fish dryers primarily focus on drying performance and energy efficiency, while limited studies integrate CFD-based airflow optimization with actual dryer experimental validation. Furthermore, large-capacity multi-layer systems with improved airflow uniformity remain insufficiently investigated in localized fish drying applications. This study aimed to optimize the design through CFD analysis and evaluate the performance of a multi-layer biomass-fired fish dryer through experimental validation. Specifically, the objectives were to: (1) integrate and evaluate baffle and exhaust vent configurations for a multi-layer biomass-fired fish dryer; (2) simulate and analyze airflow and temperature distribution within the drying chamber using CFD; (3) measure actual air temperature and velocity in the drying chamber of the dryer; and (4) evaluate the performance of the developed dryer with different fish in terms of efficiency and dried fish quality.

2. Materials And Methods

2.1. Location of the Study

The design, simulation, fabrication, and evaluation of the multi-layer biomass-fired fish dryer was conducted at the Innovations Laboratory for Process Machinery and Related Technology Development, Capiz State University – Burias Campus in the province of Capiz, from June 2023 to January 2024.

2.2. Design Improvement Modelling

The 3D model design was prepared using Dassault Systèmes SOLIDWORKS 2023. The model design of the multi-layer biomass-fired fish dryer comprised the following major components: drying cabinet, biomass holding bins, blower, biomass furnace, ash outlet, cabinet doors, drying trays, control and indicator, expanding air duct, and backdraft damper (Fig. 1). Exhaust vents and baffle assembly were added into the model design.

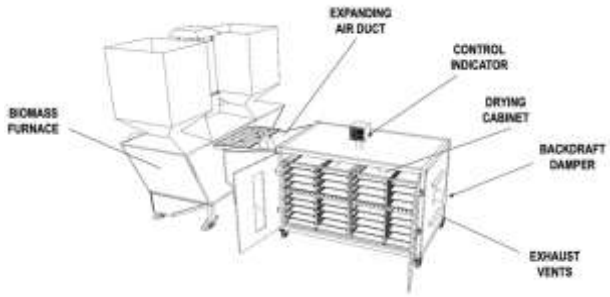

Fig. 1. Schematic layout of the multi-layer biomass-fired fish dryer.

2.3. CFD Analysis of the Design of the Multi-Layer Biomass-Fired Fish Dryer

The CFD simulations were conducted using Dassault Systèmes SOLIDWORKS Flow Simulation 2023 to find the airflow distribution and temperature uniformity within the drying chamber. The governing equations included the Navier–Stokes equations for fluid flow, the standard k–ε turbulence model for turbulence prediction, and the energy equation for heat transfer analysis. Heat transfer within the dryer was modeled primarily through forced convection and conduction. Simulations were considered converged when residual values stabilized and no significant changes in monitored temperature and airflow parameters were observed. Three CFD configurations were tested as presented in Table 1.

Table 1. Dryer configuration matrix used in CFD simulation

Configuration	Baffles	Exhaust Vents

a	✗	✓
b	✓	✗
c	✓	✓

2.3.1. Geometry and Mesh

Using the previously prepared 3D model, the different configurations were controlled by defining the initial mesh setting using basic mesh shown in Table 2. Different mesh densities were generated for each dryer configuration to ensure stable numerical solutions and adequate spatial resolution of airflow and temperature fields. The final mesh density was selected based on solution stability and consistency of airflow and temperature distributions observed during preliminary simulations. Additional local refinement was automatically applied by the software in regions with high flow gradients, particularly near the inlet, drying trays, and airflow control components. The final cell count was also refined by the software, which gave varying cell counts across different configurations.

2.3.2. Boundary Conditions and Solver Settings

Same boundary conditions were applied across all dryer configurations, as shown in Table 3. The inlet airflow was specified at 8.2 m/s, an inlet temperature of 82 °C, and a static pressure of 210 Pa, based on the heated air supplied by the biomass furnace. The airflow direction was defined as normal to the inlet surface to simulate the actual blower discharge condition.

The simulation was performed under steady-state conditions, assuming stabilized thermal and airflow behavior within the drying chamber during operation. Airflow inside the dryer was assumed to be incompressible due to the relatively low operating velocity and pressure conditions. Gravity effects were enabled in the simulation to account for buoyancy-driven airflow resulting from temperature differences within the chamber.

Table 3. Boundary conditions for CFD analysis

Parameter	Inlet Flow
Flow Velocity	8.2 m/s
Temperature	82 °C
Static Pressure	210 Pa (Gauge)
Flow Direction	Normal to the inlet surface
Turbulence Intensity	2%
Turbulence Length	0.012 m

The temperature uniformity index (TUI) of the dryer for all different configurations was taken using Equation 1:

$$TUI = \left(\frac{T_{max} - T_{min}}{T_{mean}}\right) \text{x } 100 \qquad (1)$$

2.4. Machine Fabrication

The optimized baffle assembly and exhaust vents of the multi-layer biomass-fired fish dryer were fabricated and integrated into the existing dryer. The mid-duct baffle assembly, consisting of stainless-steel grille plates, was installed within the expanding air duct to improve airflow distribution. The exhaust system, consisting of two longitudinal vents, was fabricated and installed along the cabinet sidewall to remove moist air. After assembly, the system was then inspected and tested to ensure proper operation. Fig. 2 presents the complete dryer component with enhancements.

2.5. Machine Operation

The operation of the multi-layer biomass-fired fish dryer begins with loading approximately 75 kg of rice hull into the hopper, after which the tank opener is released to allow the fuel to flow into the burner. The rice hull is ignited, and the ignition fan is activated to initiate stable combustion, followed by a brief waiting period to ensure full furnace ignition. Preheating is then performed by switching on the centrifugal fan and thermostat, raising the drying chamber temperature from ambient conditions, approximately 27 °C to 80 °C. The dryer was operated until the desired moisture content was achieved. The degree of drying depended on fish size and moisture content. After which, the dried fish are removed from the chamber and allowed to cool prior to handling and packaging.

2.6. Operational Performance Test and Product Quality Measurement

Drying air temperature (°C) was monitored using Type-K thermocouples (accuracy ±0.5 °C) installed at the air inlet

Fig. 2. Different parts of the multi-layer biomass-fired fish dryer include the following: (a) drying cabinet, (b) biomass holding bins, (c) blower, and (d) biomass furnace, (e) ash outlet, (f) cabinet doors, (g) drying trays, (h) control and indicator, (i) expanding air duct, (j) backdraft damper, (k) exhaust vents, and (l) baffle assembly.

and exhaust, and at the 11 sections of the drying chamber. The test was conducted in three trials with an eight-hour drying duration per trial, and temperature data were recorded every hour. The dryer's operational performance test was conducted to assess the applicability of the developed dryer for use in various fish types. Using four different fish, such as Anchovies, locally known as "Dilis" (Stolephorus comersonii), Boneless Anchovies, Split Round Scad locally known as "Galunggong" (Decapterus macrosoma), and Split Red Mullet locally known as "Salmonete" (Mullus surmuletus), which were freshly harvested. The performance was assessed using PNS/BAFS 344:2022 based on drying air temperature, drying rate, heating system efficiency, and fuel utilization rate. Product quality was evaluated in terms of moisture content and water activity. All instruments used in the evaluation were calibrated prior to testing, and measurements were collected under steady-state drying conditions. Drying rate (kg/hr) was determined from the mass loss of representative fish samples from each tray. The drying rate was calculated as the amount of water removed per unit drying time. Fuel utilization rate (kg/hr) was computed by dividing the total mass of rice hull consumed during each drying trial by the corresponding drying duration. Electrical energy consumption (kWh) was determined from the rated power consumption of the blower and control system multiplied by the drying duration. Heating system efficiency (HSEff) was computed using the Equation 2 below:

$$HSE = \frac{(\frac{(h_2 - h_1) * v_a}{V_{sp}}) * 60hr}{F_{fr} * HV_f} \quad (2)$$

Where:

HSE = Heating System Efficiency, %
h_2 = final enthalpy of drying air
h_1 = initial enthalpy of ambient air
V_{sp} = specific volume of drying air, m^3/kg dry air
F_{sp} = fuel feed rate, kg/hr
HV_f = heating value of fuel, kJ/kg

Initial sample weights (kg) were measured using the digital weighing scale, while moisture content was determined using the oven-drying method at 103 ± 2 °C until constant weight was achieved. During the drying operation, representative fish samples (100g) were selected from each tray to monitor moisture loss. Samples were weighed at 30-minute intervals to determine the rate of moisture content reduction throughout the drying process. The final weight (kg) of the samples was recorded. The final moisture content (%) of the dried fish was determined using the same oven-drying procedure.

A dried fish sample of 100 grams was randomly selected from each tray to evaluate the uniformity of moisture removal within the drying chamber. Representative dried fish samples (100 g) were submitted to DOST VI - RSTL (Department of Science and Technology Region VI – Regional Science and Technology Laboratory) for analysis, where water activity measurements were conducted using a calibrated water activity meter in accordance with standard laboratory procedures and at controlled room temperature.

To quantify the deviation between the Computational Fluid Dynamics (CFD) simulation results and experimental measurements, the Mean Absolute Percentage Error (MAPE) was computed. The percentage error was used to express the relative deviation of the CFD-predicted values from the experimental data and was calculated using Equation 3, where X_{CFD} and X_{Exp} represent the CFD-simulated and experimental values, respectively.

$$\text{MAPE} = \frac{1}{n}\sum(\frac{|X_{CFD} - X_{Exp}|}{X_{Exp}} x100) \quad (3)$$

Furthermore, the mean absolute difference was determined to evaluate the average absolute deviation between the two datasets, given by Equation 4, where n is the total number of observations. These statistical indicators were employed to assess the predictive accuracy and reliability of the CFD model in representing the thermal and fluid flow behavior of the system.

$$\text{Mean Absolute Difference} = \frac{1}{n}\sum_{i=1}^{n} |X_{CFD,\,i} - X_{Exp,\,i}| \quad (4)$$

2.7. Data Analysis

Data obtained were analyzed in accordance with PNS/BAFS 344:2022, using mean values, which were used to summarize machine performance parameters such as drying air temperature, drying rate, heating system efficiency, and fuel utilization rate, as well as fish quality parameters, including moisture content and water activity.

3. Results And Discussion

3.1. Simulation Outputs

The CFD simulation results revealed the velocity and temperature distribution within the drying chamber for the three tested configurations. The velocity distribution contours illustrate the airflow pattern within the system, shown in Fig. 3. The color scale on the left represents the velocity, with blue representing the lowest velocity at 0 m/s and red indicating the highest velocity at 8.3 m/s. The velocity is highest at the inlet, where the airflow enters the system. As the air moves from left to right, a gradual decrease in velocity is observed. The figure also shows that (c) exhibited the least dead zones and the most uniform air distribution across the trays. This indicates that the presence of baffles and exhaust vents enhances the uniform movement of the air inside the chamber.

In contrast, configurations (a) and (b) show uneven velocity distribution, especially inside the drying chamber. In a heat pump cabinet dryer, adjusting inlet/outlet locations and baffle angle (4 °) increased flow uniformity by ~53% and temperature uniformity by ~85% versus the original design [13]. A horizontal fluidized bed dryer with

inclined baffles removed the primary vortex, eliminated backflow, and raised the effective drying area from 21.95% (no baffles) to 57.52% and up to 83.2% with optimized baffles [25]. Moreover, Table 4 shows the CFD-based airflow data of the three (3) configurations.

The temperature distribution analysis is shown in Fig. 4. The color scale on the left ranges from 79.9 °C (blue) to 82.5 °C (red), from lowest to highest temperature zone, respectively. Configuration c exhibited minimal temperature variation across the chamber. In contrast, configurations a and b indicated noticeable temperature gradients, with the presence of localized hot and cold regions.

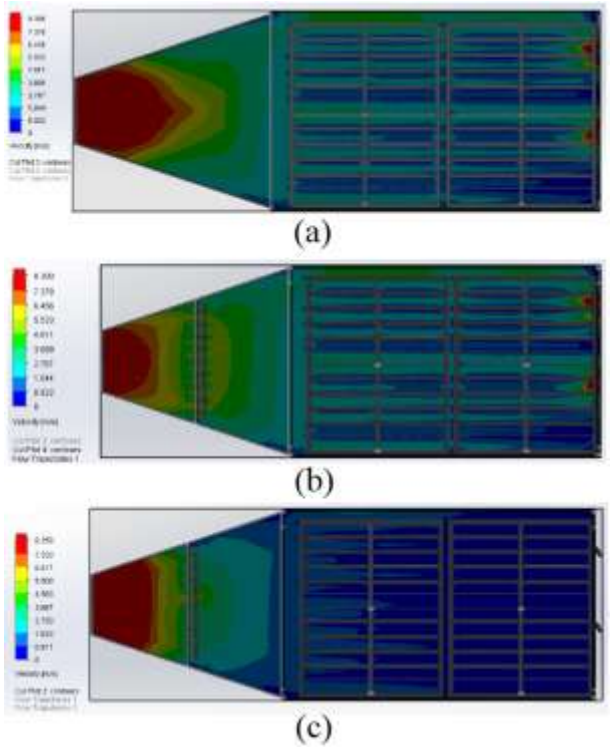

Fig. 3. Velocity distribution of all the configurations.

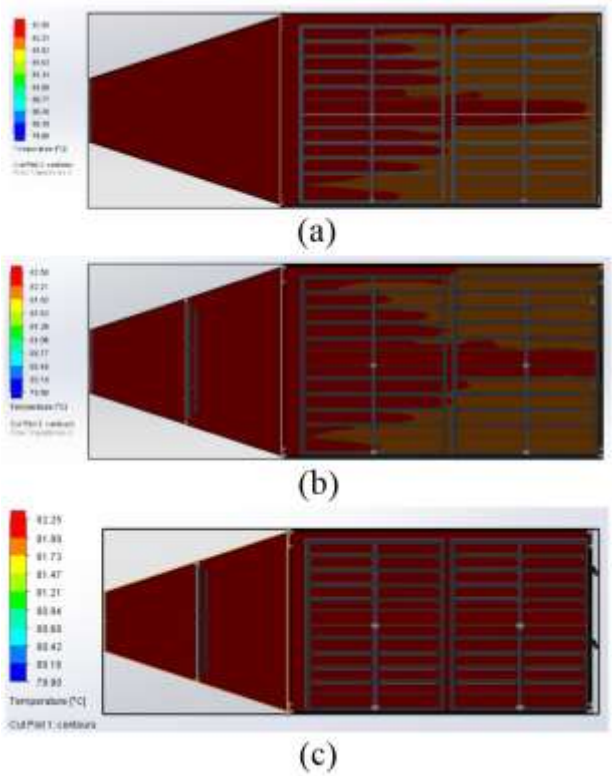

Fig. 4. Temperature distribution of all the configurations.

Table 5 shows the TUI of all the configurations. Lower TUI values indicate greater temperature uniformity. The results showed that Configuration c, with integration of baffles within the ducting system and exhaust vents, had

the lowest TUI of 0.28%, indicating the most uniform temperature throughout the drying chamber. In a heat pump cabinet dryer, varying outlet location and baffle angle led to an optimized design that improved temperature uniformity by 85.3% compared with the original configuration [13]. In solar dryers, rectangular and triangular baffles and swirlers reduced temperature gradients from 4.2–8.7 °C down to 1.0–6.8 °C, and to 1.0–3.3 °C in the best cases, effectively shrinking hot and cold spots [14, 26]. In contrast, configuration 2 had the highest TUI of 1.28%. This condition indicated the potential for uneven drying and variability in moisture removal across trays [27].

Table 4. CFD-based airflow data for different dryer configurations inside the drying chamber

Configuration	v_{min} (m/s)	v_{max} (m/s)	Mean (m/s)
a	1.143	7.526	4.335
b	1.281	7.411	4.346
c	0.917	1.829	1.373

Table 5. Summary of Temperature Uniformity Index (TUI) for different dryer configurations

Configuration	T_{min} (°C)	T_{max} (°C)	ΔT (°C)	Mean (°C)	TUI (%)
a	81.57	82.50	0.93	82.04	1.13
b	81.35	82.40	1.05	81.88	1.28
c	82.02	82.25	0.23	82.14	0.28

3.2. Description of Multi-Layer Biomass-Fired Fish Dryer

The dryer operated as a batch-type drying system. Table 6 shows the technical specifications of the multi-layer biomass-fired fish dryer used in the study.

Table 6. Technical specifications of the dryer

Parameter	Specification
Overall Dimensions	4.64 m × 1.54 m × 2.30 m
Dryer Type	Multi-layer, batch type
Number of Trays	64 units
Tray Material	Stainless steel
Tray Dimension	0.45 m × 1 m
Fan Type	Centrifugal fan
Fan Power	370 W
Airflow Capacity	92.80 m^3/min
Static Pressure	2.10 in H_2O
Heating System	Biomass furnace
Fuel Type	Rice hulls
Fuel Consumption Rate	20.8 kg/hr
Temperature Monitoring	Thermocouple with digital display

3.3. Preliminary Testing and Evaluation

3.3.1 Experimental Results

Temperature readings were obtained from the fabricated dryer at 11 representative tray locations, shown in Fig. 5.

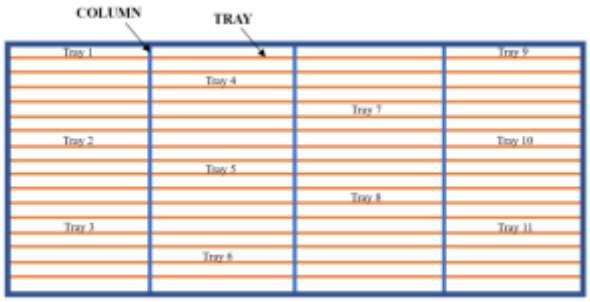

Fig. 5. Thermocouple placement inside the drying chamber layout.

Fig. 6 shows the actual drying air temperature at eleven (11) representative tray locations of the multi-layer biomass-fired fish dryer, conducted for three trials. The results show that the drying air temperature among the trays ranged from 77.98 °C to 80.12 °C, with a mean of 78.93 °C. Trays 1, 2, and 3, positioned closer to the air inlet, receive higher temperatures compared to other trays. In a study, a solar dryer having internal baffles/swirlers improves drying uniformity across trays and enhances heat distribution, lowering temperature gradients from 5.0–7.3 °C to 2.0–4.8 °C [26].

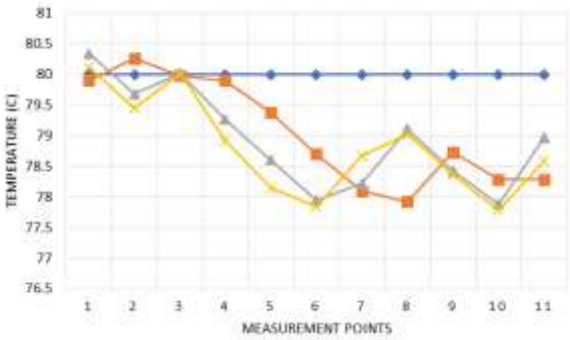

Fig. 6. Mean drying air temperature at different points inside the chamber of the multi-layer biomass-fired fish dryer

3.3.2 CFD vs Experimental Validation

The Mean Absolute Percentage Error (MAPE) between the two data is 4.05% (Table 7). Solar cabinet dryer with baffled collector tested for mango resulted in 4.35% temperature difference from the CFD-predicted results [27]. Likewise, when product moisture transport is modeled (porous domain, UDFs), CFD matches experiments within about ≤8% error in thin-layer drying of Amaranth leaves [28]. Hence, for cabinet dryers, CFD may be used to guide design and optimization, but should be followed by experimental validation.

Table 7. Comparison of CFD-predicted (configuration c) and actual temperatures at selected points

Points	CFD-Predicted Temperature (Best Configuration – Config 3) (°C)	Average Actual Temperature (3 Trials) (°C)	Absolute Percentage Error
1	82.07	80.12	2.38
2	82.21	79.80	2.93
3	82.03	80.00	2.48
4	82.18	79.36	3.43
5	82.12	78.71	4.15
6	82.01	78.16	4.69
7	82.24	78.33	4.76
8	82.09	78.68	4.15
9	82.15	78.51	4.43
10	82.05	77.98	4.96
11	82.22	78.61	4.39
Mean Temperature (°C)	82.12	78.93	4.05

3.3.3 Dryer Performance using different fish

The performance of the dryer using different types of fish was tested. Each fish type was processed to assess drying time, fuel consumption, moisture content, heating system efficiency, dried fish recovery, and fuel utilization rate, shown in Table 8. Among the fish types, the dryer was able to process split round scad with the largest input weight of 123.4 kg. The fastest drying time of 240 minutes was observed for boneless anchovies. Increasing drying temperature generally enhances moisture removal and reduces drying time, which is consistent with observations in infrared drying studies of starch-based materials [29]. In addition, among the different fish types, the boneless anchovies are the thinnest fish, which also has the lowest moisture content among the different fish samples. An experimental study on traditional sun drying found that fish thickness clearly affected drying rate: fish with a small and thin shape dried faster than thick meat species such as catfish, especially when sunlight was adequate [30]. The same study concludes that fish thickness and drying time greatly affect drying rate, and "small and thin" fish reach the target dryness sooner than thick, oily fish [30]. In a convection oven study on Tilapia zillii fillets, drying rate increased as fillet thickness decreased; optimization demonstrated that reaching ≤10% moisture at moderate temperature (≈65 °C) required fillet thickness ≤3.5 mm [31].

The highest drying rate of 18.48 kg/hr was observed when drying split round scad. It should be noted that this fish type gave the highest input weight at the dryer's full load compared with other fish types. This also implies a higher moisture load. A review of fish drying kinetics notes that higher effective moisture diffusivity increases moisture velocity within fish, improving moisture removal until equilibrium is reached [32]. Since diffusivity is highest at high moisture, this implies higher drying rates at higher moisture contents [32]. Drying boneless anchovies recorded the highest heating system efficiency of 75.17% (Fig. 7). This may be attributed to reduced drying time and lower moisture load, which minimized thermal losses. In a study where tilapia fillets were dried using a hot air dryer, it was found that cutting drying time by 33% simultaneously reduced specific energy

consumption by 60%, markedly giving higher energy efficiency of the system [33]. A study on a biomass furnace for a bed dryer reported up to 68.87% furnace efficiency during loaded operation [34]. Another study on a fluidized bed dryer achieved a heating system efficiency of 74.68% under optimized airflow and loading conditions [35].

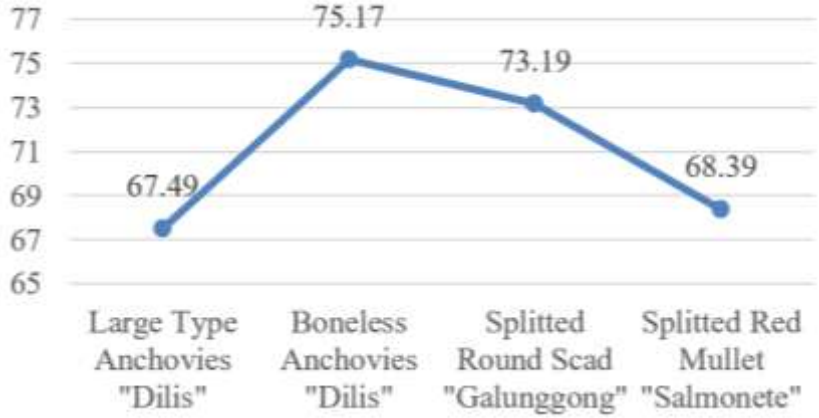

Fig. 7. Heating System Efficiency of multi-layer biomass-fired fish dryer using different fish.

Table 8. Summary of the performance evaluation of the multi-layer biomass-fired fish dryer using different fish

Fish Type	Input (kg)	Moisture Content of Dried Output (%)	Time (hr)	Drying Rate (kg/hr)	Mean Drying Temp (°C)	Fuel Utilization Rate (kg/hr)	Energy Consumption (kWh/batch)
Large Type Anchovies "Dilis"	75	21.29	4.5	16.68	75.00	21.39	1.80
Boneless Anchovies "Dilis"	50	20.44	4.0	12.48	75.00	20.31	1.60
Split Round Scad "Galunggong"	123.4	44.19	6.5	18.48	67.00	20.38	2.60
Split Red Mullet "Salmonete"	100	33.96	6.5	15.36	65.00	19.23	2.60

The variation in moisture content across the 64 trays, indicating drying uniformity within the chamber, is shown in Table 9. Boneless anchovies show the smallest range of 0.40%. In contrast, split red mullet exhibits the largest range at 3.35%. Large anchovies and split round scad show moderate ranges of 2.01% and 2.65%, respectively. In a double-layer heat pump dryer for forage seed, final seed moisture after 3 hr ranged 5.95 (tray 1) to 8.77% (tray 8), with tray-to-tray non-uniformity coefficients between 3.7% and 13.7% depending on tray position [36]. Studies using the coefficient of variation (Cv) for weight loss/moisture show that flow control devices (baffles, swirlers) can cut Cv from about 11–15% down to ~9–10%, i.e., noticeably tighter moisture spread across trays [14, 26]. The water activity of all the tested fish samples is below the maximum standard value of 0.78. Low water activity is important for food safety as it prevents microbial growth, thus extending its shelf life.

Table 9. Water activity of different fish subjected to traditional brining and mechanical drying

Fish Type	Moisture Content		Water Activity
	min	max	
Large Type Anchovies "Dilis"	19.84	21.85	0.65
Boneless Anchovies "Dilis"	20.84	21.24	0.62
Split Round Scad "Galunggong"	42.67	45.32	0.70
Split Red Mullet "Salmonete"	32.54	35.89	0.70

4. Conclusion

The findings show that the use of baffles and exhaust vents enhanced airflow distribution and temperature uniformity in the drying chamber based on CFD analysis. The experimental validation revealed that the drying conditions were stable, with air temperatures between roughly 77.5 °C and 80.8 °C and an average deviation of about 4.05% from the values predicted by CFD. This shows that with experimental validation, CFD can serve as a useful design and optimization tool for drying systems. The performance evaluation indicated that the developed dryer can be used to process different fish types, with a maximum input capacity of 123.4 kg, a highest drying rate of 18.48 kg/hr, and a maximum heating system efficiency of 75.17%. The efficiency recorded is higher than the PAES requirement of at least 50% for indirect-type dryers. The moisture content observed across trays also shows that drying is uniform and satisfactory within the chamber. The study provides an efficient solution for fish drying applications with potential for local processing operations. The system supports reduced postharvest losses and improved production stability.

5. References

[1] N. Lamarca, Fisheries Country Profile: Philippines, SEAFDEC website: http://www.seafdec.org/fisheries-country-profile-philippines/ (accessed 26.05.27).

[2] P. Udomkun, S. Romuli, S. Schock, B. Mahayothee, M. Sartas, T. Wossen, E. Njukwe, B. Vanlauwe, J. Müller, Review of solar dryers for agricultural products in Asia and Africa: An innovation landscape approach, J. Environ. Manage. 268 (2020) 110730. doi:10.1016/j.jenvman.2020.110730.

[3] J.O. Bertulfo, A.A. Roluna, J.G. Carillo, L.B.C. Silong, Design and development of solar dryer for local seaweeds (Kappaphycus spp.), Proc. Int. Exch. Innov. Conf. Eng. Sci. 8 (2022) 96–102. doi:10.5109/5909071.

[4] S.S. Marine, M.A. Sayeed, P.P. Barman, R. Begum, M. Hossain, M.T. Alam, Traditional methods of fish drying: An explorative study in Sylhet, Bangladesh, Int. J. Fishery Sci. Aquac. 2 (1) (2015) 028–035.

[5] Y. Deng, Y. Wang, Q. Deng, L. Sun, R. Wang, L. Ye, S. Tao, J. Liao, R. Gooneratne, Fungal diversity and mycotoxin contamination in dried fish products in Zhanjiang market, China, Food Control 121 (2021) 107614. doi:10.1016/j.foodcont.2020.107614.

[6] J. Maïworé, L.T. Ngoune, M.K. Koumba, I. Metayer, D. Montet, N. Durand, Determination of bacterial population and the presence of pesticide residues from some Cameroonian smoked and dried fish, Sci. Afr. 13 (2021) e00886. doi:10.1016/j.sciaf.2021.e00886.

[7] N. Thapa, Ethnic fermented and preserved fish products of India and Nepal, J. Ethn. Foods 3 (1) (2016) 69–77. doi:10.1016/j.jef.2016.02.003.

[8] M.R. Nukulwar, V.B. Tungikar, A review on performance evaluation of solar dryer and its material for drying agricultural products, Mater. Today Proc. 46 (1) (2021) 345–349. doi:10.1016/j.matpr.2020.08.354.

[9] S.K. Shittu, A. Umar, Development of a charcoal fired fish dryer for small scale processors, Niger. J. Eng. 27 (2) (2020) 27–34.

[10] G. Yang, X. Yang, C. Li, et al., Numerical study on the uniform distribution of flow field of airflow dryer, Heliyon 10 (2024). doi:10.1016/j.heliyon.2024.e29439.

[11] S. Mondal, S. Dutta, P. Pande, V. Naik-Nimbalkar, Intensify staple fibre drying by optimizing air distribution in multistage convective dryer using CFD, Chem. Eng. Process. Process Intensif. (2022). doi:10.1016/j.cep.2022.108807.

[12] C. Wang, Y. Pei, Z. Mu, et al., Simulation analysis of 3-D airflow and temperature uniformity of paddy in a laboratory drying oven, Foods 13 (2024). doi:10.3390/foods13213466.

[13] Y. Gai, Z. Zhang, X. Wang, The influence of various layouts of internal baffles on air distribution in heat pump cabinet dryers, Int. Commun. Heat Mass Transf. (2024). doi:10.1016/j.icheatmasstransfer.2024.108209.

[14] H. Kidane, I. Farkas, J. Buzás, Optimizing solar drying chamber performance: Taguchi analysis of uniformity enhancement methods, Int. J. Energy Res. (2025). doi:10.1155/er/5061778.

[15] P. Huo, Y. Wang, Numerical simulation and optimization of airflow distribution in ceramic drying room, Heat Transfer Eng. 46 (2024) 192–206. doi:10.1080/01457632.2023.2301158.

[16] A. Benhamza, A. Boubekri, A. Atia, T. Hadibi, M. Arıcı, Drying uniformity analysis of an indirect solar dryer based on computational fluid dynamics and image processing, Sustain. Energy Technol. Assess. 47 (2021) 101466. doi:10.1016/j.seta.2021.101466.

[17] I.A.A. Jabbar, A.A. Mohammed, H.F. Mahmood, Optimizing air flow and temperature distribution in a greenhouse solar dryer using computational fluid dynamics, J. Adv. Res. Numer. Heat Transfer (2025). doi:10.37934/arnht.29.1.1626.

[18] M.A.A. Rahmat, A. Ibrahim, M.A.A. Ishak, U. Syafiq, K.M. Al-Aribe, Numerical investigation of thermal and airflow profiles in diverse solar dryer chamber configurations, Case Stud. Therm. Eng. (2025). doi:10.1016/j.csite.2025.106612.

[19] X. Chen, D. Wang, Y. Wang, et al., CFD design and testing of an air flow distribution device for microwave infrared hot-air rolling-bed dryer, Biosyst. Eng. (2024). doi:10.1016/j.biosystemseng.2024.08.005.

[20] C.H. Bao, L.T. Dat, N.D. Khoa, H.M. Quang, T.H. Chieu, et al., Application of computational fluid dynamics in examining the filtration efficacy of fine and coarse particles in a baffle integrated-vertical ventilation duct, Proc. Int. Exch. Innov. Conf. Eng. Sci. (2022). doi:10.5109/5909101.

[21] P.V. Alfiya, S. Murali, D.A.S. Delfiya, M.P. Samuel, Design and development of biomass-fueled convective dryer for marine products: energy, exergy, environmental, and economic (4E) analysis, Biomass Convers. Biorefinery 15 (2024) 12031–12042. doi:10.1007/s13399-024-06001-6.

[22] M. Dongmo, C.V.A. Kazé, J.P.D. Sayouba, Design and construction of a hybrid gas and biogas dryer for fruits, vegetables, meat and fish, E3S Web Conf. (2022). doi:10.1051/e3sconf/202235403008.

[23] S.K. Shittu, A. Umar, Development of a charcoal fired fish dryer for small scale processors, Niger. J. Eng. 27 (2) (2020) 27–34.

[24] K. Elavarasan, V. Verma, B. Shamasundar, Development of prototype solar-biomass hybrid dryer and its performance evaluation using salted fish (Cynoglossus spp.), Indian J. Fish. 64 (2017). doi: 10.21077/ijf.2017.64.special-issue.76242-17.

[25] S. Handayani, E. Yohana, M. Tauviqirrahman, A.G. Rahman, M.E. Yulianto, K. Choi, Performance improvement of continuous horizontal fluidised bed dryer based on computational fluid dynamics, Results Eng. (2023). doi:10.1016/j.rineng.2023.100972.

[26] H. Kidane, I. Farkas, J. Buzás, Enhancing the drying uniformity in solar drying systems: computational and experimental study, Int. J. Thermofluids (2025). doi:10.1016/j.ijft.2025.101408.

[27] E.A. Tesema, M.A. Delele, S.W. Fanta, F.B. Masrie, M.A. Workie, E. Tsegaye, Experimental and numerical approaches: performance optimization of a baffled solar cabinet dryer for mango slices, Ethiop. Int. J. Eng. Technol. (2025). doi:10.59122/184dfd15.
[28] A.K. Babu, G. Kumaresan, V.A.A. Raj, S.B.V. Surya, Numerical simulation of heat pump thin layer drying of amaranth leaves, Energy Sources A Recover. Util. Environ. Eff. 45 (2023) 9383–9395. doi:10.1080/15567036.2023.2232737.
[29] J.O. Bertulfo, P.T.M.B. Butao, J.M. Sordilla, Mathematical modelling and thin layer drying of sago starch using infrared dryer, Proc. Int. Exch. Innov. Conf. Eng. Sci. 8 (2022) 134–140. doi:10.5109/5909081.
[30] N. Azizah, N.A. Asfiyanti, M. Hasibuan, M. Jannah, R. Gustari, R.S. Hasibuan, The effect of fish thickness on dryness level and time for drying fish, Int. J. Nat. Sci. Eng. (2022). doi:10.23887/ijnse.v5i3.41891.
[31] O. Sanda, D.A. Sanda, E.A. Taiwo, C.O. Aremu, J.O. Ojediran, B.S. Fakinle, Mathematical modelling of the drying kinetics and optimization of process conditions for Tilapia zillii fillets dried in a convection oven, Trop. J. Nat. Prod. Res. 7 (6) (2023). doi:10.26538/tjnpr/v7i6.29.
[32] S.A.O. Adeyeye, An overview of fish drying kinetics, Nutr. Food Sci. (2019). doi:10.1108/nfs-10-2018-0296.
[33] K. Komanee, A. Namkhat, S. Pumchumpol, U. Teeboonma, Effect of temperature and air velocity on kinetics and energy efficiency of fish fillets drying, J. Adv. Res. Fluid Mech. Therm. Sci. 132 (2) (2025) 117–130. doi:10.37934/arfmts.132.2.117.
[34] I. Putra, G. Safruloh, Z. Frisdan, J. Karyadi, B. Purwantana, A. Telaumbanua, D. Ayuni, Performance test of the biomass furnace for bed dryer using various agriculture wastes, IOP Conf. Ser. Earth Environ. Sci. 1038 (2022) 012023. doi:10.1088/1755-1315/1038/1/012023.
[35] Sukmawaty, Hardiansyah, A. Priyati, D.A. Setiawati, Syahrul, Analysis of heating system on fluidized bed dryer for corn, IOP Conf. Ser. Earth Environ. Sci. 355 (1) (2019) 012090. doi:10.1088/1755-1315/355/1/012090.
[36] G. Guangbin, X. Kaixuan, Y. Qichao, Z. Yuangyang, L. Liansheng, Flow field and drying process analysis of double-layer drying chamber in heat pump dryer, Appl. Therm. Eng. (2022). doi:10.1016/j.applthermaleng.2022.118261.